**Title: Reliable Readout of Mixture Components from Small Populations of Anterior Piriform Cortical Neurons**

Abbreviated title: Odorant-Mixture Coding in the Anterior Piriform Cortex

Sapir Penker[1], Tamar Licht[1], Katharina T. Hofer[1], and Dan Rokni[1]*

1. Department of Neurobiology, School of Medicine and IMRIC, The Hebrew University, Jerusalem, Israel

* Corresponding author: Dan Rokni dan.rokni@mail.huji.ac.il

Number of pages: 19

Number of figures: 5

Number of tables: 0

Number of words in abstract: 213

Number of words in introduction: 633

Number of words in discussion: 899

The authors declare no competing financial interests

**Acknowledgements**

This work was funded by a European Research Council Starting Grant (755764 - COFBMIX). We are grateful to Yoram Ben-Shaul, Mati Joshua, Adi Mizrahi, and Ithai Rabinowitch for commenting on early versions of the manuscript, and to members of the Rokni lab for stimulating discussions.

**Abstract**

Airborne chemicals emitted by multiple objects, mix in the air prior to reaching the nose, complicating the recognition of specific odors of interest. The olfactory system is therefore faced with the task of segmenting odor mixtures to identify objects in the presence of rich and often unpredictable backgrounds. The piriform cortex is thought to be the site of object recognition and scene segmentation, yet the nature of its responses to odorant mixtures is largely unknown. In this study, we asked two related questions. 1) How do mixture representations in the piriform cortex relate to the representations of individual mixture components? And 2) Can the identity of individual mixture components be read out from mixture representations in the piriform cortex? To answer these questions, we recorded single unit activity in the piriform cortex of naïve mice while sequentially presenting single odorants and their mixtures. We find that the magnitude of piriform cortical responses increases with added mixture components, and that the responses of individual neurons are typically well explained by a normalization model. Finally, we show that mixture components can be identified from piriform cortical activity by pooling responses of a small population of neurons. These results suggest that piriform cortical representations are well suited to perform figure-background segmentation without the need for learning.

**Significance statement**

Olfactory research has mainly focused on the encoding and processing of individual isolated odors. However, stimuli in nature are never in isolation. It is currently unknown how the olfactory system processes complex stimuli and how it identifies specific odors embedded in varying backgrounds. In this study we analyzed piriform cortical responses to odorant mixtures. We find that mixture responses can typically be described with a simple normalization model. We also show that the activity of small populations of piriform neurons and often even individual neurons can provide sufficient information for identifying odorants embedded within background mixtures. This suggests that segmentation of target odors from the background is a built-in feature of piriform cortical processing.

## Introduction

The odorants emitted by different objects in the environment mix in the air before reaching the nose. Each of these objects in itself will typically emit tens to thousands of odorants that become its olfactory signature. Natural inputs into the olfactory system are therefore rich odorant mixtures that require segmentation in order for useful information to be extracted. Mixture segmentation is complicated by the overlapping representations of odorants by olfactory sensory neurons (Malnic et al., 1999; Rubin and Katz, 1999; Araneda et al., 2000; Kajiya et al., 2001; Abaffy et al., 2006; Grosmaitre et al., 2009; Soucy et al., 2009). Similar to the auditory system (and unlike the visual system), a single sensory neuron may be simultaneously activated by odorants originating from multiple objects (Brungart et al., 2001; McDermott, 2009). Behavioral testing has indeed shown that increased overlap in odorant representations is related to increased difficulty of scene segmentation (Rokni et al., 2014). Temporal separation between the arrival of different odors into the nose may aid in segmentation either via mechanisms of adaptation (Wilson, 2003; Kadohisa and Wilson, 2006a; Linster et al., 2007; Vinograd et al., 2017) or by readout of synchronous activity in the olfactory bulb (Hopfield, 1995; Brody and Hopfield, 2003), however such separation is not guaranteed and mice can indeed segment odorant mixtures without temporal separation (Rokni et al., 2014). Due to the overlapping representations of odorants by olfactory receptors, scene segmentation requires integration of multiple receptor channels. Such integration takes place in the piriform cortex where individual neurons receive inputs from multiple receptor channels (Apicella et al., 2010; Davison and Ehlers, 2011; Ghosh et al., 2011; Miyamichi et al., 2011; Sosulski et al., 2011). This feature of piriform connectivity is the basis for several models of scene segmentation (Li and Hertz, 2000; Mathis et al., 2016; Grabska-Barwińska et al., 2017; Singh et al., 2019).

In order to understand how the piriform cortex segments odorant mixtures one would want to have an understanding of how neurons in the piriform cortex represent odorant mixtures, and specifically how these representations relate to the representations of individual mixture components. Several studies have reported sublinear mixture responses in olfactory cortex (Lei et al., 2006; Yoshida and Mori, 2007; Stettler and Axel, 2009). Non-linear interactions between mixture components already take place at the level of the olfactory epithelium (Kurahashi et al., 1994; Duchamp-Viret et al., 2003; Oka et al., 2004; Takeuchi et al., 2009; Xu et al., 2019; Zak et al., 2019). While these interactions make odorant representations highly background dependent, they may actually increase the amount of information carried by a population of sensory neurons about mixture components (Reddy et al., 2018). At the level of the olfactory bulb, lateral inhibitory circuits may further modify odor representations in a background-dependent manner (Yokoi et al., 1995; Urban, 2002; Aungst et al., 2003; Arevian et al., 2008; Fantana et al., 2008), although at least at the input level, intraglomerular circuits seem to be the main player in shaping olfactory bulb representations (McGann et al., 2005). The piriform cortex integrates these non-linear odor representations from the olfactory bulb and utilizes local recurrent circuitry to generate representations that presumably support segmentation (Poo and Isaacson, 2009, 2011; Franks et al., 2011; Miura et al., 2012; Suzuki and Bekkers, 2012; Roland et al., 2017; Bolding and Franks, 2018). Currently however, the nature of these mixture representations in the piriform cortex is still poorly understood. One can still not predict a mixture response from the responses to the individual odorants. Additionally, how information about mixture components is coded and can be readout from piriform cortical activity is not known.

To answer these questions, we systematically characterized mixture representations in the piriform cortex and analyzed their ability to convey information about individual mixture components, at both the single neuron, and population levels.

**Materials and Methods:**

All experimental procedures were performed using approved protocols in accordance with institutional (Hebrew University IACUC) and national guidelines.

Data acquisition: Young adult male c57bl6 mice (10-14 weeks old, Envigo) were anesthetized (Ketamine/Medetomidine 75 and 1 mg/kg, respectively), and were restrained in a stereotaxic device (Model 940, David Kopf Instruments). The skin was removed from the scalp and a small craniotomy was made over the anterior piriform cortex (1.5 mm anterior and 2.8 mm lateral to bregma). A metal plate was attached to the skull with dental acrylic and was used to hold mice at the electrophysiological rig. Normal body temperature (37 C) was maintained with a heating pad (Harvard Apparatus). A single tungsten electrode (A-M systems, 10-12 MOhm) was lowered into the piriform cortex with a micromanipulator (Sutter Instruments). Signals from the electrode were band pass filtered (300-5000 Hz), amplified (X1000, A-M systems 1800), and sampled at 20KHz and digitized with 16-bit precision (National Instruments PCIe-6351). All analog signals were displayed and saved for offline analysis using custom-made software in LabVIEW (National Instruments). Injections of a TRITC-labeled 10Kd dextran (500 nL, Molecular probes cat#D1817, 10mg/ml) were used to verify piriform cortical targeting.

Odors were presented using a custom-made, computer-controlled, odor presentation machine that maintains constant flow and allows mixing of odors without mutual dilution (Rokni et al., 2014). The following 8 odorants were used (all from Sigma Aldrich, CAS numbers in parentheses): 1. isobutyl propionate (540-42-1), 2. 2-ethyl hexanal (123-05-7), 3. ethyl valerate (539-82-2), 4. propyl acetate (109-60-4), 5. isoamyl tiglate (41519-18-0), 6. phenethyl tiglate (55719-85-2), 7. citral (5392-40-5), 8. ethyl propionate (105-37-3). All odorants were diluted to 10% in diethyl phthalate (84-66-2), and then further diluted 8 fold in air. Odors were presented into a mask that fit the mouse's snout at a rate of 1 l/min and were cleared from the mask by vacuum that was set to create an outward flow of 1 l/min (Figure 1A). A third port of the mask was connected to a mass flow sensor (Honeywell AWM3300) to monitor respiration. For each recording session, a set of 4 odorants was chosen (initially randomly and later fixed to odorants 1, 3, 5, and 7). All 15 combinations of these 4 odorants were then presented with randomized order (typically repeating ~30 times each). Odors were presented for 1.5 s with an inter-trial interval of 20 s.

Data analysis: Action potentials were detected offline using custom-written code in Matlab, and were then sorted using MClust (David Redish). Only units that had less than 1 in 1000 spikes to have occurred within a 3 ms refractory period were considered as single units and further analyzed. Respiratory signals were low-pass filtered with a moving average window of 250 ms. Inhalation onsets were defined as zero crossings with negative slope. All neural responses were aligned to the first inhalation onset following odor onset. PSTHs were generated with 1 ms bins and filtered with a 50 ms window Gaussian moving average. Response significance was tested by comparing the mean spike rate during a 3 second response period to the mean spike rate in a 3 second period with no odor, using the Wilcoxon ranksum test with a

threshold p-value of 0.01. All responses are shown as baseline-subtracted spike rates. To fit normalization models, data was fit to equation 1 using the lsqcurvefit function in Matlab. Fit quality was assessed with the coefficient of determination ($R^2$).

Receiver operating characteristic (ROC) analysis was performed using the perfcurve function in Matlab. For each neuron, ROC analysis was performed separately to test the detectability of each odorant. The reported performance of each neuron is the best across the 4 odorants. The performance reported for each odorant is the best across all neurons. Shuffled controls were created by shuffling the stimulus labels for all neurons and obtaining a distribution of 224 auROC values (4 odorants X 56 neurons). Performance is reported as above control if the auROC was above all shuffled controls.

For population analysis, we generated a pseudo-population by pooling neurons from different experiments in which we used the same 4 odorants (odorants 1, 3, 5, and 7). Linear classifiers were realized as logistic regressions and were fit using the fitclinear function in Matlab. Classifiers were cross-validated by creating a test set that was not used for training. Each test set included one randomly selected response from each neuron to each of the 15 odor combinations. A training set that did not include the testing trials was then generated by randomly selecting trials from each neuron for each odor combination. The training set included 10,000 trials of each of the 15 stimuli for most analyses. For the analysis of temporal resolution, the training set was increased to 100,000. The reported performance for the classifiers is the mean over 100 iterations. For assessing the effect of population size on classification accuracy, we gradually removed inputs from the classifier by sequentially removing the neuron with the minimal absolute weight.

**Results**

We recorded the responses of single neurons in the anterior piriform cortex of naïve anesthetized mice, to all possible combinations of 4 odorants (4 single odorants, 6 pairs, 4 triplets, 1 mix of 4, Figure 1A-D). Various sets of 4 odorants were used (from 8 odorants available in the odor presentation machine). Because the isolation of single-unit activity is critical for the following analysis, we recorded neural activity using single tungsten electrodes which provide a much higher signal to noise ratio than most multi-channel systems and allows better separation of single-unit spikes. We recorded from 56 well-isolated neurons of which 53 responded significantly to at least one of the 15 odor combinations. Odor stimuli were presented using a mask that fit the mouse's snout and were cleared with constant negative pressure (Figure 1A). The mask was also connected to a mass flow sensor for continuous monitoring of respiration. Dye injections in the same coordinates that were used for recordings (1.5 mm anterior and 2.8 mm lateral to Bregma, 4.5mm ventral), verified anterior piriform cortical targeting (Figure 1B). All odor responses were aligned to the first inhalation onset following odor valve opening (Figure 1C,D).

The basal firing of cortical neurons was typically very low (1.9 ± 0.05 Hz, mean ± SEM, Figure 1E), and both basal firing and odor responses were typically strongly modulated by respiration (Figure 1D, F, & G). Odor responses were predominantly positive (increases in firing rate) with only 18% showing mild decreases in firing rate (Figure 1H). This may be an underestimate of inhibitory inputs as most neurons had a basal firing rate of less than 1 spike per second, rendering our analysis less sensitive to inhibition. Of the responding neurons, most responded significantly to more than one of the individual odorants (Figure 2A). We first asked whether adding odorants to a mixture increases overall responses in the piriform

cortex. Analyzing response statistics across all responsive neurons, we found that the fraction of significant responses ($p<0.01$) was positively correlated with the number of mixture components ($r=0.98$, $p=0.017$, Figure 2B). The simplest model for response integration is a linear model in which a neuron's response to a mixture is equal to the sum of its responses to the mixture components. To test for linearity of odorant integration, we compared mixture responses of all neurons to the linear sum of the responses to individual mixture components (Figure 2C). Most mixture responses were below the linear prediction (Figure 2C,D), however mixture responses were correlated with the linear prediction (Figure 2E). As a measure of sublinearity, we calculated the mean slope of the relationship between the observed and linearly predicted mixture responses for each neuron. The median slope of the linear fits was 0.5 (Figure 2F). Taken together, these analyses show that in agreement with previous studies, the vast majority of piriform cortical responses to odorant mixtures increase with added mixture components and that this increase is sublinear.

While a linear model is useful as a minimal model for analyzing the general increase in piriform responses with added components, a neuron's firing rates are limited by their intrinsic properties and by inhibitory inputs, and therefore cannot increase linearly. Indeed, piriform cortical odor representations have been shown to be strongly affected by local inhibitory circuits that perform a computation akin to normalization (Bolding and Franks, 2018). We therefore fitted mixture responses with a model that is similar to the one used to describe mixture responses in olfactory sensory neurons (Mathis et al., 2016):

$$R = Rmax\left(\frac{2}{1+e^{-s\cdot LP}} - 1\right) \qquad (eq.1)$$

In this model, R is the neuron's response to a mixture, LP is the linear sum of the individual component responses, Rmax is the neuron's maximal response, and s is a parameter that sets the initial slope of the function (at LP=0). Rmax and s are the two fitted parameters. We found that this model explains mixture responses well for most neurons (Figure 3A1-A3). Some neurons however, could not be properly explained with such a model (Figure 3A4). The normalization model could account for most of the variance ($R^2$ above 0.5) in 30/53 (57 %) of the cells (Figure 3B). The neurons that could not be well explained with this model (low $R^2$) showed little increase in their responses as mixture components were added as assessed by the slope of the linear fit (Figure 3C). Whether these neurons represent a separate neuronal subtype is unclear, yet the quality of the normalization fit was not correlated with spike waveform, basal firing rate or preferred respiratory phase of firing (Figure 3D-F). These results indicate that piriform neuronal responses can often be explained by a simple normalization model.

One of the suggested tasks that the piriform cortex is presumed to solve is figure-background segmentation. It was recently suggested that individual piriform neurons may be able to detect target odors in a background-invariant manner by pooling inputs from multiple glomeruli (Mathis et al., 2016; Singh et al., 2019). We therefore asked whether the presence of individual odorants in mixtures can be extracted from the activity of individual piriform neurons. We used receiver operator characteristic (ROC) analysis to test whether the responses to mixtures that contain a specific target odorant are discriminable from responses to mixtures that do not contain the target odorant (Figure 4). For each neuron, we assessed discriminability for all 4 odorants in the experiment and quantified it with the area under the ROC curve (auROC). We assessed each neuron's discrimination power with its best discriminated odorant (Figures 4A-B). Many neurons yielded high levels of discriminability with 54/56 (96%) neurons performing better than shuffled-labels controls and 11/56 (20%) cells having an auROC of above 0.8. The

discriminability for each odorant based on its single best neuron ranged from auROC of 57 to 99.7 and averaged at 79 (Figure 4C). Mice detect target odorants from background mixtures in about 500 ms (Rokni et al., 2014). We therefore analyzed how single neuron target detection is affected by the time window over which responses are calculated. Responses integrated within a window of less than 200 ms from stimulus onset were not informative about target odorants and the auROC curve plateaued for most neurons between 800 and 1600 ms (Figure 4D). The longer integration windows are presumably more informative about target odorants due to increased spike counts and signal to noise ratio, but they may also be more informative because they cover the right epoch in which action potentials carry the most information about the presence of the target odorant. To analyze for the latter, we repeated the ROC analysis with 200 ms windows that were shifted in time (Figure 4E). 12/56 neurons had at least one 200 ms epoch for which the auROC was above 0.8. The auROC as a function of time for these 12 neurons was highly correlated with the shape of their PSTHs in response to the target odorants. These analyses indicate that single piriform neurons may be highly informative about the presence of a target odorant within a mixture, and that detection can be performed in time scales that match previous behavioral measurements.

We next analyzed the ability to detect target odorants from the activity of piriform cortical populations. We pooled data from all cells stimulated with a specific set of 4 odorants (37 cells) to create a pseudo-population. We then trained linear classifiers (realized as logistic regressions) to classify trials according to the presence of each individual odorant. Classifiers were cross-validated by constructing a test set that included a single response from each neuron to each of the 15 odor combinations. Test set responses were not included in the training set. The mean classification accuracy across target odorants was 88 % correct (99% for odorant 1, 88% for odorant 2, 86% for odorant 3, and 78% for odorant 4). The performance of the classifiers typically decreased for richer mixtures, starting from an average performance of 94±2 % for single odorants and decreasing to 82±6% for mixtures with 4 components (Figure 5A). To assess the number of neurons required to detect individual odorants from mixtures, we trained classifiers using sub-populations (Figure 5B). We started with the entire population and gradually removed the neuron with the minimal absolute weight. On average across odors, 6 neurons were sufficient to reach a performance level above 90 % of the level achieved with the entire population (1 neuron for odorant 1, 8 for odorant 2, 7 for odorant 3, and 6 for odorant 4). To relate classidfier decoding to behavioral decision speed, we next tested how classifier performance depends on the response integration time (Figure 5C). Classifier performance degraded only for one target odorant when decreasing the integration time from 3 to 1 s, but degraded sharply for all target odorants when decreasing the integration window below 500 ms. The average performance across odors with 500 ms integration time was 77±5 %. Finally, we tested whether spike timing carries any information beyond what is carried by the mean firing rates. We trained classifiers with temporal inputs at varying temporal resolution (Figure 5D). Decreasing time bins below 500 ms yielded over-fitted models that performed badly on test trials. Even when the total response duration was lowered to 1 second and the number of training trials was increased 100 fold, time bins below 500 ms yielded over-fitted models (not shown). This indicates that the anterior piriform cortex does not use a temporal code to convey information about the presence of target odors embedded in background mixtures. Together, these analyses show that the detection of target odorants against background mixtures can be reliably achieved with a small number of piriform neurons.

## Discussion

We recorded from single neurons in the anterior piriform cortex of naïve anesthetized mice and describe their responses to odorant mixtures. We used receiver operator characteristic (ROC) analysis, and linear classifiers to describe the availability of information regarding mixture components in single neuron, and population activity, respectively. Our main findings are that (i) piriform responses can be described with a normalization model that relates mixture responses to the linear sum of individual component responses, and (ii) individual odorants can be reliably detected from mixtures by the firing of small neuronal populations in the piriform cortex.

Previous analyses of mixture representations in the piriform cortex have found that sub-linear summation of odorant responses is the common case, although examples of supra-linear summation have also been demonstrated (Yoshida and Mori, 2007; Stettler and Axel, 2009). Similar variability in odorant summation has also been found in the anterior olfactory nucleus (Lei et al., 2006). Our analysis shows that combining multiple mixture responses of individual neurons uncovers a mathematical relationship between them. The normalization model may explain some of the variability in previous studies as responses far below the saturation level ($R_{max}$ in eq 1) may appear linear while greater responses will be sublinear. Normalization has been found in many cortical regions and has been proposed as a canonical computation performed by cortical circuits that allows them to encode variables monotonically without saturating (Carandini and Heeger, 2012). Normalization was also demonstrated in the drosophila antennal lobe, the insect brain region equivalent to the mammalian olfactory bulb (Olsen et al., 2010). Several mechanisms may contribute to the sublinear summation of odorant responses. These include interactions between odorants at the olfactory epithelium (Kurahashi et al., 1994; Duchamp-Viret et al., 2003; Oka et al., 2004; Grossman et al., 2008; Takeuchi et al., 2009; Reddy et al., 2018; Xu et al., 2019; Zak et al., 2019), processing in the olfactory bulb (Giraudet et al., 2002; Linster and Cleland, 2004; Tabor et al., 2004; Lin et al., 2006), and further normalization within piriform cortex, implemented by local inhibition. Inhibitory circuits within the piriform cortex have indeed been shown to play a major role in shaping piriform representations (Poo and Isaacson, 2009, 2011; Franks et al., 2011; Bolding and Franks, 2018). In our data, most neurons were well fit by the normalization model, however, it is important to note that some neurons were not. These cells were mostly cells that did not increase their activity when mixture components were added, and it is possible that we only probed them with stimuli that push them to their saturated response levels. Although the quality of fit to the normalization model was not correlated with any electrophysiological signature that might have been indicative of cell type (baseline firing, phase preference, and spike waveform), we cannot rule out the possibility that different neuronal populations integrate mixture components differently. Indeed principal neurons in the piriform cortex include subpopulations that differ in their localization across layers, biophysical properties, projection targets, and possibly tuning width (Suzuki and Bekkers, 2006, 2011; Zhan and Luo, 2010; Diodato et al., 2016).

The finding that single piriform neurons may be sufficient to detect target odorants against background mixtures is in line with recently proposed models for target odorant detection from mixtures (Mathis et al., 2016; Singh et al., 2019). In these models, individual glomeruli are not informative about the presence of any specific odorant, but pooling information from a population of glomeruli, supports accurate classification. As piriform neurons receive inputs from multiple receptor channels, they are poised to be suitable for this classification. Similar findings have been described in the insect olfactory system, where mushroom body Kenyon cells (but not antennal lobe projections neurons) reliably report the presence of a single odorant in a mixture (Shen et al., 2013). Using linear classifiers, we showed that target odorant

detection can be improved by pooling inputs from a small population of neurons. Providing classifiers with temporal inputs yielded over-fitted models indicating that the anterior piriform cortex probably does not use a temporal code to represent odorants embedded in mixtures. This is in line with previous work indicating that the anterior piriform cortex primarily employs a rate code to project odor information (Miura et al., 2012; Haddad et al., 2013). The inputs for the classifiers were pseudo-populations pooled from multiple experiments. Pooling responses from multiple experiments removes noise-correlations and therefore is expected to improve classifier performance (Zohary et al., 1994). It should be noted however that previous measurements have found very little noise correlations in the piriform cortex during odor sampling (Miura et al., 2012). Importantly, the mice we recorded from, were naïve to the odorants and were never trained to detect any of them. The fact that piriform cortical neurons in naïve mice already show an impressive ability of target detection, suggests that this ability requires little or no learning. It will be intriguing to study to what extent training on a mixture segmentation task improves this ability.

In this study we focused on the ability to detect mixture components, however, mixtures of odorants that are emitted from individual objects typically create a unified percept in which the individual components are not identified (Jinks and Laing, 2001; Kadohisa and Wilson, 2006b; Barnes et al., 2008; Gottfried, 2010; Wilson and Sullivan, 2011; Howard and Gottfried, 2014). It will be interesting for future studies to investigate how normalized mixture representations support unified object percepts.

**References**

Abaffy T, Matsunami H, Luetje CW (2006) Functional analysis of a mammalian odorant receptor subfamily. Journal of Neurochemistry 97:1506–1518.

Apicella A, Yuan Q, Scanziani M, Isaacson JS (2010) Pyramidal cells in piriform cortex receive convergent input from distinct olfactory bulb glomeruli. J Neurosci 30:14255–14260.

Araneda RC, Kini AD, Firestein S (2000) The molecular receptive range of an odorant receptor. Nat Neurosci 3:1248–1255.

Arevian AC, Kapoor V, Urban NN (2008) Activity-dependent gating of lateral inhibition in the mouse olfactory bulb. Nat Neurosci 11:80–87.

Aungst JL, Heyward PM, Puche AC, Karnup SV, Hayar A, Szabo G, Shipley MT (2003) Centre–surround inhibition among olfactory bulb glomeruli. Nature 426:623–629.

Barnes DC, Hofacer RD, Zaman AR, Rennaker RL, Wilson DA (2008) Olfactory perceptual stability and discrimination. Nat Neurosci 11:1378–1380.

Bolding KA, Franks KM (2018) Recurrent cortical circuits implement concentration-invariant odor coding. Science 361:eaat6904.

Brody CD, Hopfield JJ (2003) Simple networks for spike-timing-based computation, with application to olfactory processing. Neuron 37:843–852.

Brungart DS, Simpson BD, Ericson MA, Scott KR (2001) Informational and energetic masking effects in the perception of multiple simultaneous talkers. The Journal of the Acoustical Society of America 110:2527–2538.

Carandini M, Heeger DJ (2012) Normalization as a canonical neural computation. Nat Rev Neurosci 13:51–62.

Davison IG, Ehlers MD (2011) Neural circuit mechanisms for pattern detection and feature combination in olfactory cortex. Neuron 70:82–94.

Diodato A, Ruinart de Brimont M, Yim YS, Derian N, Perrin S, Pouch J, Klatzmann D, Garel S, Choi GB, Fleischmann A (2016) Molecular signatures of neural connectivity in the olfactory cortex. Nature Communications 7:12238.

Duchamp-Viret P, Duchamp A, Chaput MA (2003) Single olfactory sensory neurons simultaneously integrate the components of an odour mixture. European Journal of Neuroscience 18:2690–2696.

Fantana AL, Soucy ER, Meister M (2008) Rat Olfactory Bulb Mitral Cells Receive Sparse Glomerular Inputs. Neuron 59:802–814.

Franks KM, Russo MJ, Sosulski DL, Mulligan AA, Siegelbaum SA, Axel R (2011) Recurrent Circuitry Dynamically Shapes the Activation of Piriform Cortex. Neuron 72:49–56.

Ghosh S, Larson SD, Hefzi H, Marnoy Z, Cutforth T, Dokka K, Baldwin KK (2011) Sensory maps in the olfactory cortex defined by long-range viral tracing of single neurons. Nature 472:217–220.

Giraudet P, Berthommier F, Chaput M (2002) Mitral Cell Temporal Response Patterns Evoked by Odor Mixtures in the Rat Olfactory Bulb. J Neurophysiol 88:829–838.

Gottfried JA (2010) Central mechanisms of odour object perception. Nat Rev Neurosci 11:628–641.

Grabska-Barwińska A, Barthelmé S, Beck J, Mainen ZF, Pouget A, Latham PE (2017) A probabilistic approach to demixing odors. Nat Neurosci 20:98–106.

Grosmaitre X, Fuss SH, Lee AC, Adipietro KA, Matsunami H, Mombaerts P, Ma M (2009) SR1, a Mouse Odorant Receptor with an Unusually Broad Response Profile. J Neurosci 29:14545–14552.

Grossman KJ, Mallik AK, Ross J, Kay LM, Issa NP (2008) Glomerular activation patterns and the perception of odor mixtures. Eur J Neurosci 27:2676–2685.

Haddad R, Lanjuin A, Madisen L, Zeng H, Murthy VN, Uchida N (2013) Olfactory cortical neurons read out a relative time code in the olfactory bulb. Nat Neurosci 16:949–957.

Hopfield JJ (1995) Pattern recognition computation using action potential timing for stimulus representation. 376:33–36.

Howard JD, Gottfried JA (2014) Configural and Elemental Coding of Natural Odor Mixture Components in the Human Brain. Neuron 84:857–869.

Jinks A, Laing DG (2001) The analysis of odor mixtures by humans: evidence for a configurational process. Physiol Behav 72:51–63.

Kadohisa M, Wilson DA (2006a) Olfactory Cortical Adaptation Facilitates Detection of Odors Against Background. Journal of Neurophysiology 95:1888–1896.

Kadohisa M, Wilson DA (2006b) Separate encoding of identity and similarity of complex familiar odors in piriform cortex. Proceedings of the National Academy of Sciences 103:15206–15211.

Kajiya K, Inaki K, Tanaka M, Haga T, Kataoka H, Touhara K (2001) Molecular Bases of Odor Discrimination: Reconstitution of Olfactory Receptors that Recognize Overlapping Sets of Odorants. J Neurosci 21:6018–6025.

Kurahashi T, Lowe G, Gold GH (1994) Suppression of odorant responses by odorants in olfactory receptor cells. Science 265:118–120.

Lei H, Mooney R, Katz LC (2006) Synaptic integration of olfactory information in mouse anterior olfactory nucleus. J Neurosci 26:12023–12032.

Li Z, Hertz J (2000) Odour recognition and segmentation by a model olfactory bulb and cortex. Network 11:83–102.

Lin DY, Shea SD, Katz LC (2006) Representation of Natural Stimuli in the Rodent Main Olfactory Bulb. Neuron 50:937–949.

Linster C, Cleland TA (2004) Configurational and Elemental Odor Mixture Perception Can Arise from Local Inhibition. J Comput Neurosci 16:39–47.

Linster C, Henry L, Kadohisa M, Wilson DA (2007) Synaptic adaptation and odor-background segmentation. Neurobiology of Learning and Memory 87:352–360.

Malnic B, Hirono J, Sato T, Buck LB (1999) Combinatorial Receptor Codes for Odors. Cell 96:713–723.

Mathis A, Rokni D, Kapoor V, Bethge M, Murthy VN (2016) Reading Out Olfactory Receptors: Feedforward Circuits Detect Odors in Mixtures without Demixing. Neuron 91:1110–1123.

McDermott JH (2009) The cocktail party problem. Curr Biol 19:R1024-1027.

McGann JP, Pírez N, Gainey MA, Muratore C, Elias AS, Wachowiak M (2005) Odorant Representations Are Modulated by Intra- but Not Interglomerular Presynaptic Inhibition of Olfactory Sensory Neurons. Neuron 48:1039–1053.

Miura K, Mainen ZF, Uchida N (2012) Odor representations in olfactory cortex: distributed rate coding and decorrelated population activity. Neuron 74:1087–1098.

Miyamichi K, Amat F, Moussavi F, Wang C, Wickersham I, Wall NR, Taniguchi H, Tasic B, Huang ZJ, He Z, Callaway EM, Horowitz MA, Luo L (2011) Cortical representations of olfactory input by trans-synaptic tracing. Nature 472:191–196.

Oka Y, Omura M, Kataoka H, Touhara K (2004) Olfactory receptor antagonism between odorants. The EMBO Journal 23:120–126.

Olsen SR, Bhandawat V, Wilson RI (2010) Divisive normalization in olfactory population codes. Neuron 66:287–299.

Poo C, Isaacson JS (2009) Odor Representations in Olfactory Cortex: “Sparse” Coding, Global Inhibition, and Oscillations. Neuron 62:850–861.

Poo C, Isaacson JS (2011) A Major Role for Intracortical Circuits in the Strength and Tuning of Odor-Evoked Excitation in Olfactory Cortex. Neuron 72:41–48.

Reddy G, Zak JD, Vergassola M, Murthy VN (2018) Antagonism in olfactory receptor neurons and its implications for the perception of odor mixtures. eLife Available at: https://elifesciences.org/articles/34958 [Accessed August 2, 2018].

Rokni D, Hemmelder V, Kapoor V, Murthy VN (2014) An olfactory cocktail party: figure-ground segregation of odorants in rodents. Nat Neurosci 17:1225–1232.

Roland B, Deneux T, Franks KM, Bathellier B, Fleischmann A (2017) Odor identity coding by distributed ensembles of neurons in the mouse olfactory cortex. eLife 6:e26337.

Rubin BD, Katz LC (1999) Optical Imaging of Odorant Representations in the Mammalian Olfactory Bulb. Neuron 23:499–511.

Shen K, Tootoonian S, Laurent G (2013) Encoding of Mixtures in a Simple Olfactory System. Neuron.

Singh V, Tchernookov M, Balasubramanian V (2019) What the odor is not: Estimation by elimination. bioRxiv:568626.

Sosulski DL, Bloom ML, Cutforth T, Axel R, Datta SR (2011) Distinct representations of olfactory information in different cortical centres. Nature 472:213–216.

Soucy ER, Albeanu DF, Fantana AL, Murthy VN, Meister M (2009) Precision and diversity in an odor map on the olfactory bulb. Nat Neurosci 12:210–220.

Stettler DD, Axel R (2009) Representations of odor in the piriform cortex. Neuron 63:854–864.

Suzuki N, Bekkers JM (2006) Neural Coding by Two Classes of Principal Cells in the Mouse Piriform Cortex. J Neurosci 26:11938–11947.

Suzuki N, Bekkers JM (2011) Two layers of synaptic processing by principal neurons in piriform cortex. J Neurosci 31:2156–2166.

Suzuki N, Bekkers JM (2012) Microcircuits Mediating Feedforward and Feedback Synaptic Inhibition in the Piriform Cortex. J Neurosci 32:919–931.

Tabor R, Yaksi E, Weislogel J-M, Friedrich RW (2004) Processing of Odor Mixtures in the Zebrafish Olfactory Bulb. J Neurosci 24:6611–6620.

Takeuchi H, Ishida H, Hikichi S, Kurahashi T (2009) Mechanism of olfactory masking in the sensory cilia. The Journal of General Physiology 133:583–601.

Urban NN (2002) Lateral inhibition in the olfactory bulb and in olfaction. Physiology & Behavior 77:607–612.

Vinograd A, Livneh Y, Mizrahi A (2017) History-Dependent Odor Processing in the Mouse Olfactory Bulb. J Neurosci 37:12018–12030.

Wilson DA (2003) Rapid, Experience-Induced Enhancement in Odorant Discrimination by Anterior Piriform Cortex Neurons. Journal of Neurophysiology 90:65–72.

Wilson DA, Sullivan RM (2011) Cortical processing of odor objects. Neuron 72:506–519.

Xu L, Li W, Voleti V, Hillman EMC, Firestein S (2019) Widespread Receptor Driven Modulation in Peripheral Olfactory Coding. bioRxiv:760330.

Yokoi M, Mori K, Nakanishi S (1995) Refinement of odor molecule tuning by dendrodendritic synaptic inhibition in the olfactory bulb. Proc Natl Acad Sci U S A 92:3371–3375.

Yoshida I, Mori K (2007) Odorant Category Profile Selectivity of Olfactory Cortex Neurons. J Neurosci 27:9105–9114.

Zak JD, Gautam R, Vergassola M, Murthy VN (2019) Antagonistic odor interactions in olfactory sensory neurons are widespread in freely breathing mice | bioRxiv. Available at: https://www.biorxiv.org/content/10.1101/847525v1.abstract [Accessed December 15, 2019].

Zhan C, Luo M (2010) Diverse Patterns of Odor Representation by Neurons in the Anterior Piriform Cortex of Awake Mice. J Neurosci 30:16662–16672.

Zohary E, Shadlen MN, Newsome WT (1994) Correlated neuronal discharge rate and its implications for psychophysical performance. Nature 370:140–143.

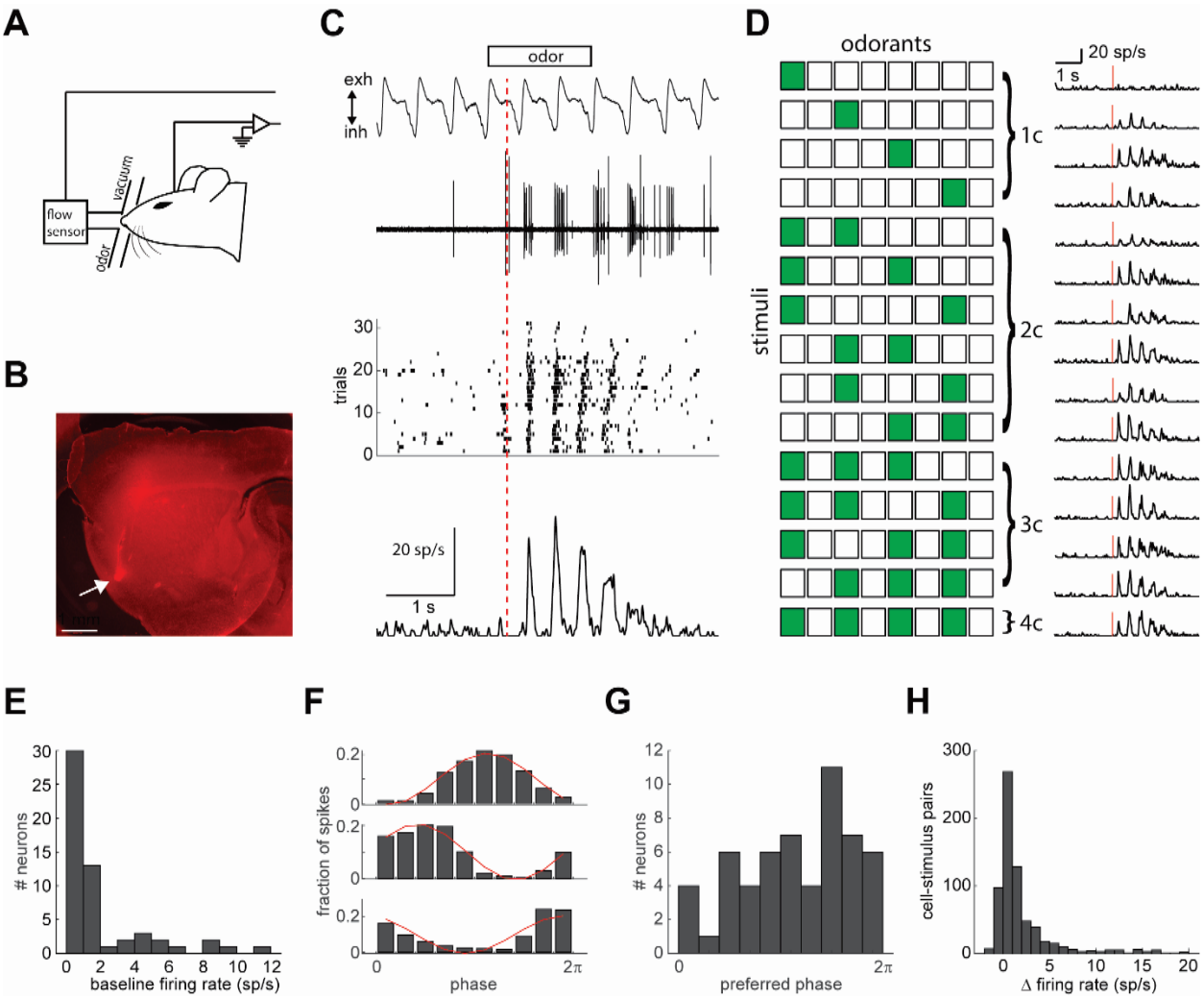


**Figure 1.** Mixture responses in piriform cortex. **A.** Schematic of experimental setup. **B.** A sagittal section of a brain that was injected with a 10Kd rhodamine at the same coordinates used for recordings. Arrow marks the injection site in the anterior piriform cortex. **C.** Example raw data (respiration and electrophysiology), raster plot, and PSTH in response to a mixture of 2 odorants (od 3&5). **D.** Responses of the same cell shown in C to all combinations of 4 odorants. **E.** Histogram of baseline firing rates. **F.** Fraction of spikes as a function of respiratory phase shown for 3 example cells. Red line shows a cosine fit. **G.** Histogram of preferred baseline firing phase. **H.** Histogram of change in firing rate in response to odor stimulation.

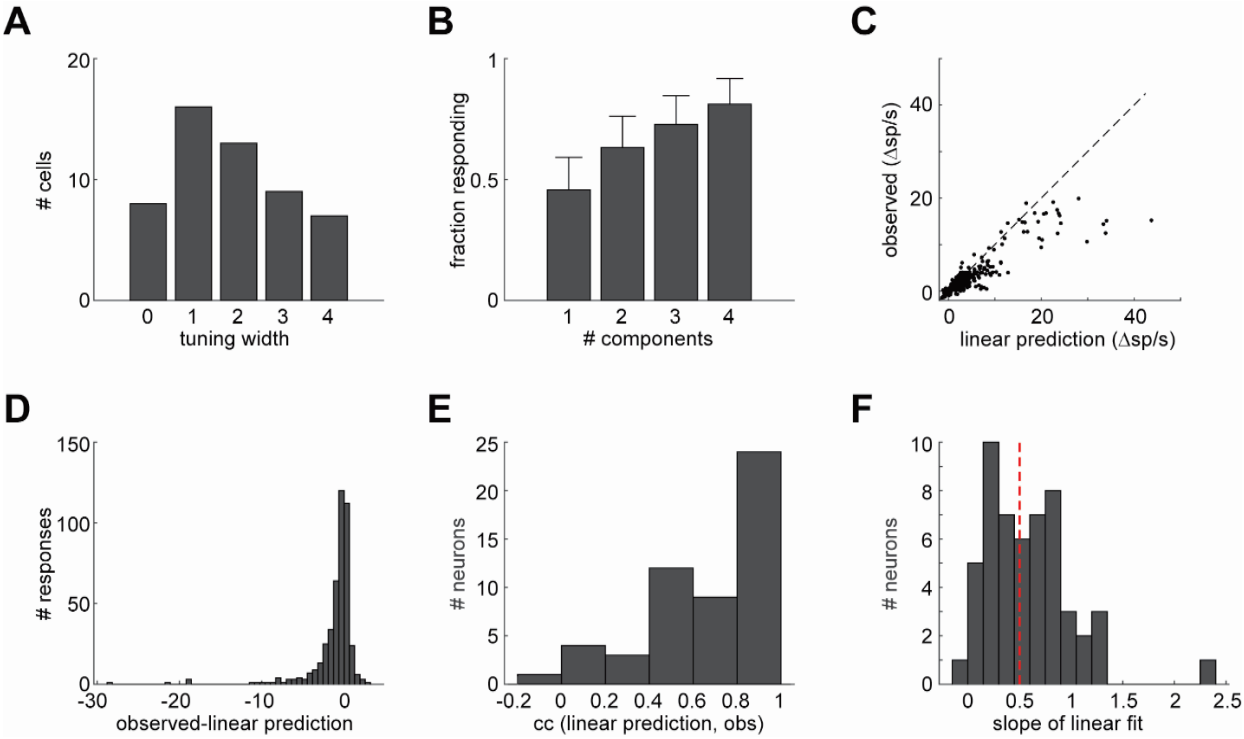


**Figure 2.** Sublinear summation of odor responses. **A.** Histogram of the tuning width of all cells that responded to at least one of the fifteen stimuli (53/56). Tuning width is defined as the number of single odorants that elicited a statistically significant response ($p<0.01$). **B.** Fraction of significant responses ($p<0.01$) as a function of the number of odorants in the mixture. **C.** Observed responses (firing rate) vs the linear sum of individual odorant responses. Responses of all cell-mixture pairs are shown. Dashed line is the unity line. **D.** Histogram of the differences between observed and linearly predicted mixture responses. **E.** Histogram of correlation coefficients between the linearly predicted and observed responses. **F.** Histogram of the slopes obtained in linear fits to the relationship between the linearly predicted and observed responses. Red dashed line indicates the median slope.

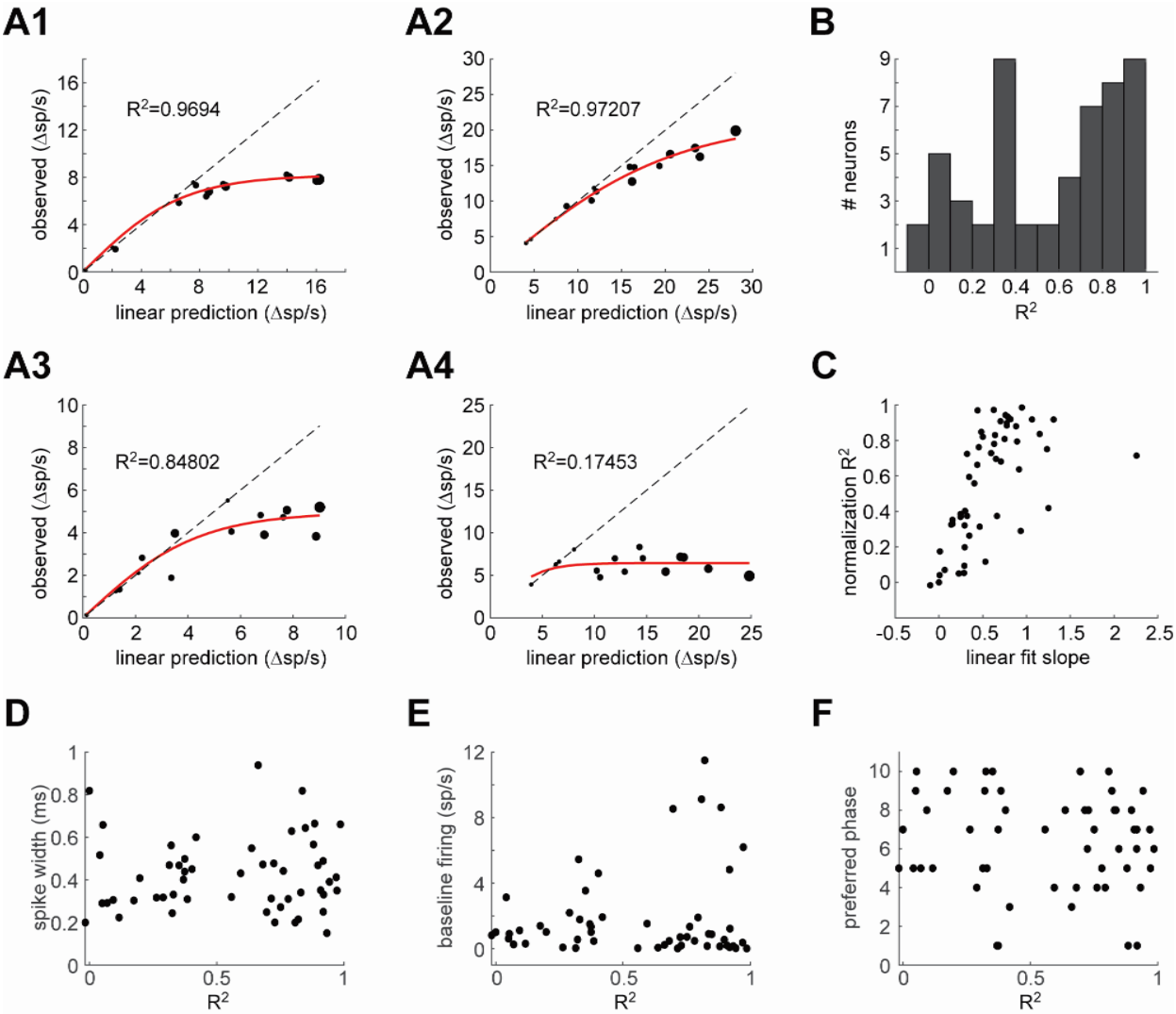


**Figure 3.** A normalization model explains most piriform mixture responses. **A1-4.** Examples from 4 cells showing the relationship between the linearly predicted and observed responses. The size of the symbol indicates the number of odorants in the mixture. Red line shows the fit to equation 1. Dashed line is the unity line. **B.** Histogram of the coefficients of determination ($R^2$) of the fits to equation 1 obtained from all cells. **C.** The coefficients of determination plotted against the slope of a linear fit. **D-F.** Spike width (D), baseline firing rate (E), and Preferred respiratory phase (F), plotted against the coefficient of determination obtained in the fit to equation 1.

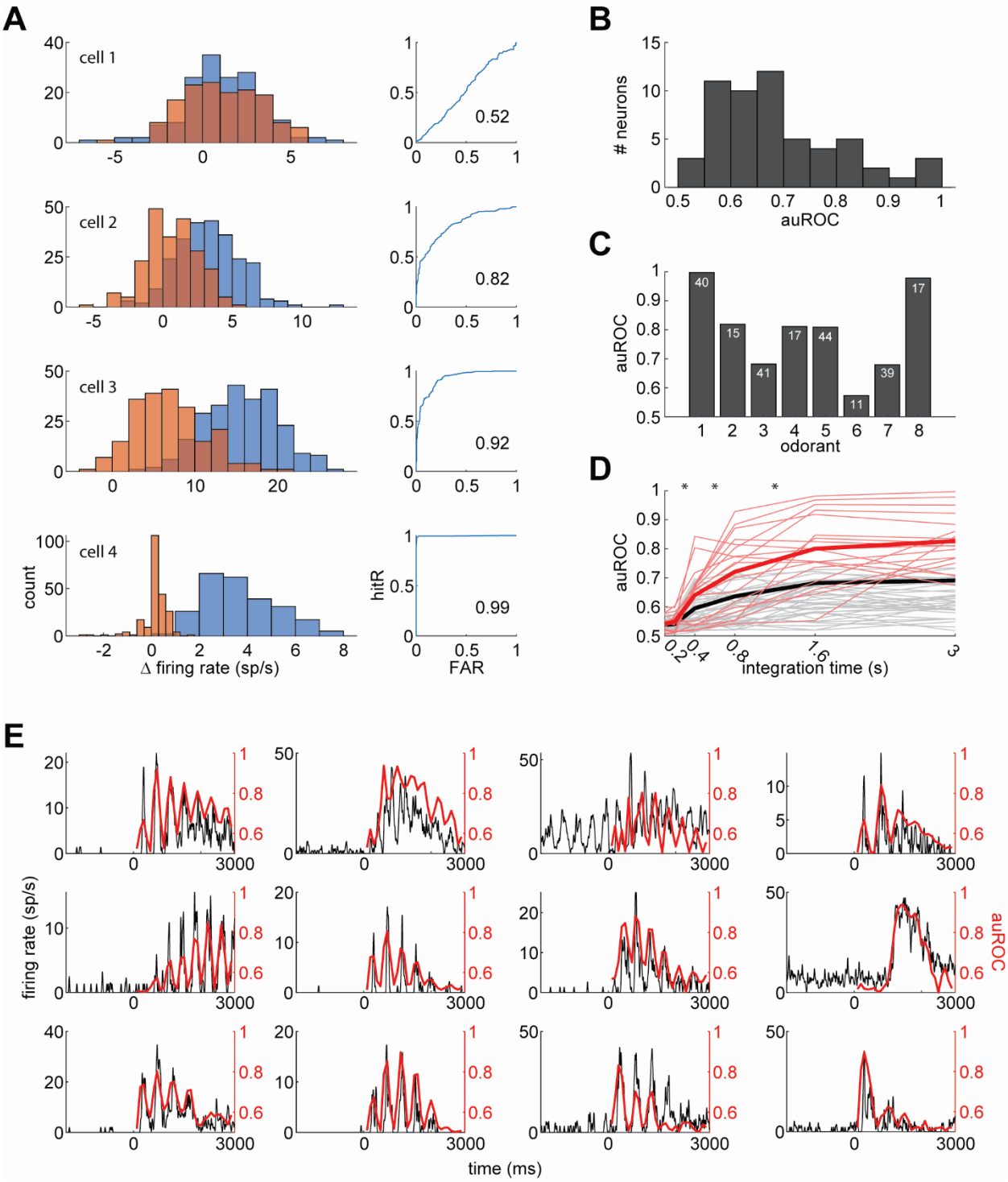


**Figure 4.** Detection of target odorants with single neurons. **A.** The ROC analysis of 4 example cells. Firing rate histograms are shown on left (blue – all mixtures including a particular odorant, orange – all mixtures excluding the odorant). Panels on the right show hit rate vs false alarm rate as the decision boundary is shifted (numbers indicate the area under the curve). **B.** Histogram of the area under the ROC curve. The highest value for each neuron (across the 4 odorants) is included. **C.** The maximal area under the curve obtained for each odorant. The number of neurons tested with each odorant is indicated. **D.** The area

under the curve for each cell (with its best odor) as a function of the duration of response integration. Low performing cells (never reaching performance of 0.8) are shown in gray, high performing cells are shown in red. The mean of all cells (black) and the high performing cells (red) are shown in thick lines. **E.** The area under the curve using a sliding 200 ms integration window as a function of the time of integration along the response (red) superimposed with the PSTH in response to the detected odorant (black). 12 high performing neurons are shown.

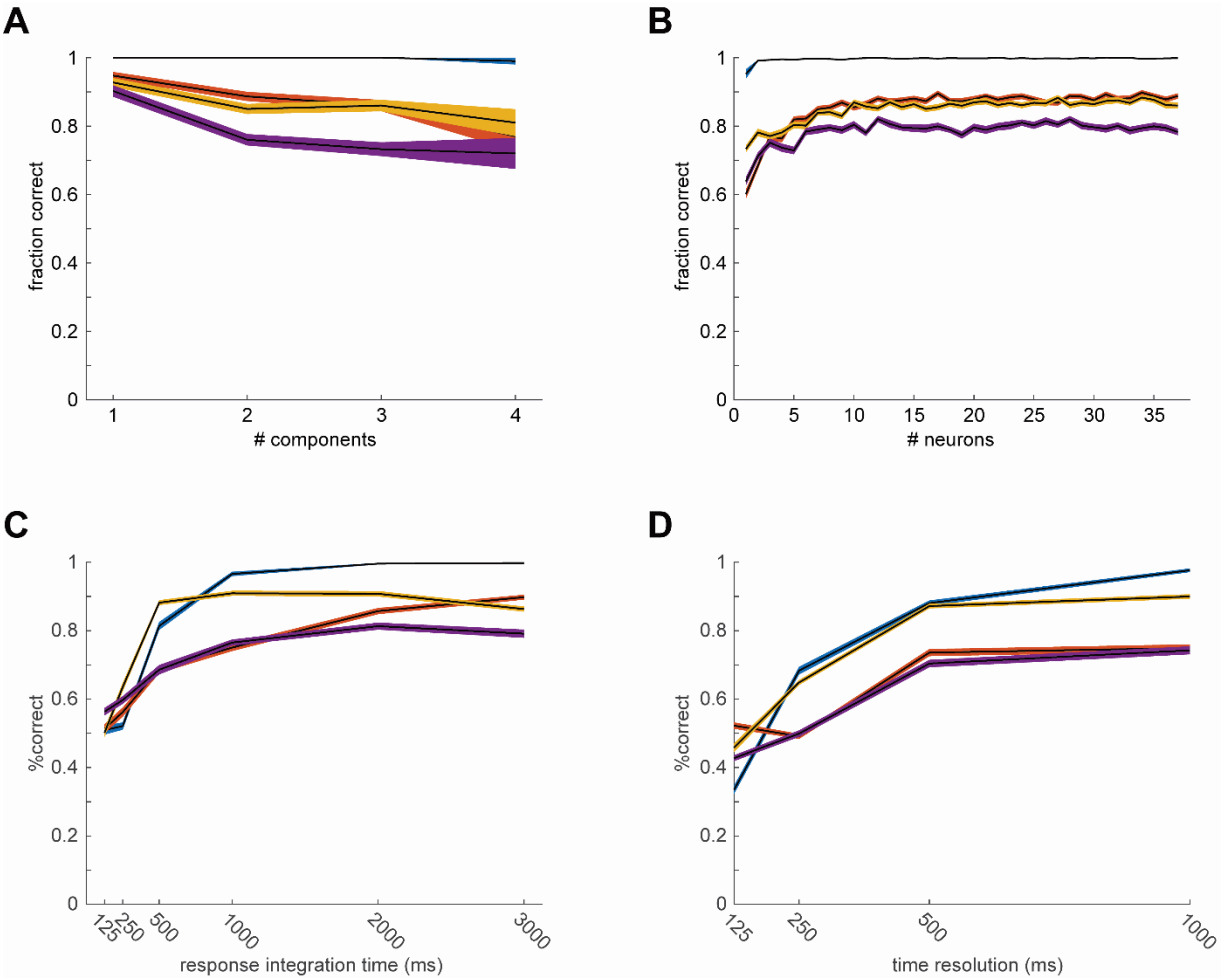


**Figure 5.** Detection of target odorants with pseudo-populations. In all panels black lines show the average performance for each odorant, and the color-shaded areas show the standard error of the mean. The different colors represent the 4 different odorants (blue – od1, red – od3, yellow – od5, purple – od7). **A.** Performance of the linear classifiers as a function of the number of odorants in the mixture. **B.** Performance of the classifiers as a function of the number of neurons used as input. **C.** Performance of the classifiers as a function of the duration of the response integration window. **D.** Performance of the classifiers as a function of temporal resolution.